Natural Hazards (2006) 37:153–167
DOI 10.1007/s11069-005-4661-0

Landslides and Rainfall Characteristics Analysis in Taipei City during the Typhoon Nari Event

FAN-CHIEH YU[1], TIEN-CHIEN CHEN[2,★], MEEI-LING LIN[3], CHIEN-YUAN CHEN[4] and WEN-HAI YU[4]

[1]*Department of Soil and Water Conservation, National Chung Hsing University, 250 Guoguang Road, 402, Taichung, Taiwan, ROC;* [2]*Department of Soil and Water Conservation, National Pingtung University of Science and Technology, 1 Hseuh Fu Road, Neipu, 912, Pingtung, Taiwan, ROC;* [3]*Department of Civil Engineering, National Taiwan University, Sec. 4, 1 Roosevelt Road, 106, Taipei, Taiwan, ROC;* [4]*National Science and Technology Center for Disaster Reduction, Sec. 2, 3F, 106, Ho Ping E. Road, 106, Taipei, Taiwan, ROC*

Abstract. The severe Typhoon Nari ended on September 15, 2001 with a high-intensity and high-accumulation storm that dumped up to 1249 mm of rain in Taipei City, Taiwan. The high-intensity and high-accumulation event caused flooding and triggered more than 400 soils slips and debris flows and large, complex landslides. Detailed information on 63 events, including rainfall, initiation time, and magnitude of landslides were documented and analyzed to identify the landslides and rainfall characteristic in Taipei City during Typhoon Nari. The result reveals that slump, slide, and debris flow events are associated with the situation of high-intensity or high-accumulation rainfall. The rainfall intensity-duration condition resulted in smaller magnitude and shallow failures. Medium to massive landslide were mainly related to the high-accumulation rainfall. A landslide regionalization process based on rainfall, geomorphologic and geologic characteristics is proposed. Results of the proposed process show good agreement with landslide events observed in the Taipei City during Typhoon Nari.

Key words: landslides, rainfall intensity, rainfall accumulation, GIS, regionalization, Taipei City, Taiwan

1. Introduction

More and more landslide warning systems were studied by using remote sensing, ground-base monitoring, or rain gauge station methods (Caine, 1980; Cannon and Ellen, 1985; Keefer *et al.*, 1987; Wieczorek, 1987; Sugiyama *et al.*, 1995; Ba Mamoudou and Sharon, 1998; Singhroy *et al.*, 1998; Fan *et al.*, 2002; Jan, 2002). Because there is insufficient understanding of the landslide and rainfall characteristics, the systematized landslide warning system has some difficulties in applying in practice. In the paper, sixty-three landslide data including rainfall, initiation time, and

★ Author for correspondence: E-mail: tcchen@npust.edu.tw

magnitude of landslides were documented and analyzed to identify the landslides and rainfall characteristic in Taipei City during Typhoon Nari. The study focused on the types and magnitude of landslides relating to the peak intensity rainfall and the cumulative rainfall. Six typhoons and a tropical troposphere event induced torrential rains on September 5, 2001 were introduced for the study on rainfall characteristic in Taipei City.

A regionalization process is proposed that could group the areas in same rainfall and landslide characteristics through the rainfall characteristics, geomorphologic and geologic analysis. The applicability of the proposed process was also demonstrated using events in Taipei City during Typhoon Nari.

2. Landslide Characteristics Analysis

There were 427 landslide events induced by Typhoon Nari in Taipei City. We collected landslide data from the field investigation and the official report of police department, 63 events including the nearest landslide initiating-time were documented and verified. Rain gauge stations introduced to the calculation of corresponding rainfall are shown in Figure 1. Antecedent rainfall (one week cumulative rainfall before typhoon hit Taiwan on September 15, 2001) of these stations are summarized in Table I. According to the data, the antecedent rainfall is minor and could be neglected in this event.

We calculated rainfall intensity and effective accumulation at the most possible initiation moment of landslide and illustrated in Figure 2. There are 27 cases out of the 63 landslide cases ($\sim$43%) related to high intensity rainfall with rainfall intensity exceeding 30 mm/h. There are 30 cases ($\sim$48%) with high effective accumulation (>500 mm) but with the intensity less than 10 mm/h.

Lag times between landslide initiation and peak rainfall intensity are summarized in Table II. The table reveals that there are 27 out of the 63 cases of landslide initiated during -1 to 3 h prior to the peak intensity rainfall. Sixteen cases initiated in the period of peak intensity rainfall. The period of peak intensity rainfall is defined as the time within -1 to 1 h of peak intensity rainfall to envelop the possibility of delay when event cases were registered. Moreover, there are 36 cases of landslide initiated after 3 h of the peak intensity rainfall. Summarizing the analysis, it reveals that both of high intensity rainfall and cumulative rainfall are the critical factors to trigger a landslide.

It also shows in Table II that there were 46 cases with landslide areas smaller than 1,500 m^2. Only 4 cases were over 15,000 m^2, however, all of them were within 4 h period of peak intensity rainfall. It still had 15 landslide cases initiated beyond 10 h after the peak intensity rainfall, nevertheless, those magnitude are classified as medium or small. In general, the landslide

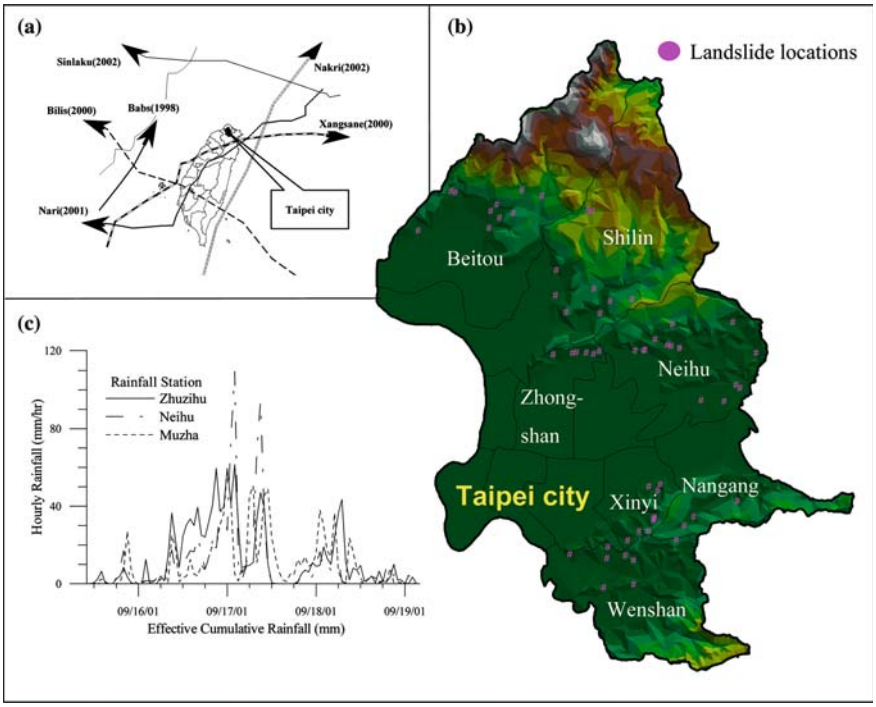

Figure 1. (a) Paths of typhoons hit Taiwan during 1998–2002. (b) Three rainfall characteristic sub-regions in Taipei City. (c) Rainfall hourly records of rainfall stations for Typhoon Nari (2001).

Table I. Antecedent rainfalls of Typhoon Nari, the rainfalls were calculated using the record of rain gauge stations for one week before the typhoon hit Taiwan on September 15, 2001

Rain gauge station	Guandu	Shipal	Tianmu	Shilin	Xinyi	Waishuangxi	Dazhi	Neihu	Nangang	Muzha
Antecedent rainfall (mm)	0.05	0.07	0.08	0.15	0.11	0.27	0.07	0.13	0.12	0.26

inducing by high intensity rainfall is smaller in magnitude. Most of the medium to massive landslides will distribute beyond 2 h after the peak intensity rainfall.

Table III shows the lag time between landslide initiating to peak intensity rainfall relating to the types of landslides. Landslide types were recognized in field and classified as rockfall, wedge failure, plane failure, erosion, debris slide, block slide, and circular failure seven types. As showed in Table III, the types concentrated on erosion, debris slide, block slide, and circular failure, however the distribution were random in all

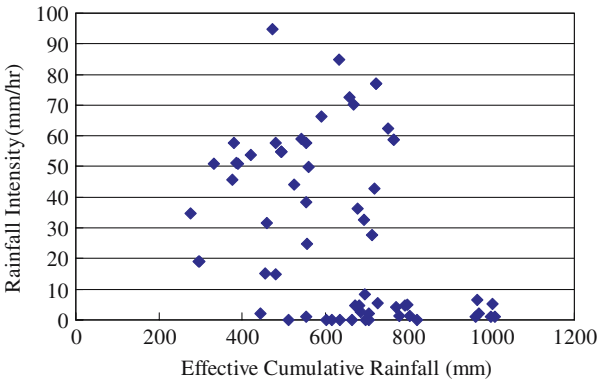

Figure 2. Sixty-three rainfall intensity versus effective cumulative rainfalls in Taipei City during Typhoon Nari. Both of rainfalls were calculated at or before the period of landslides initiating.

Table II. Number of counts as events occurred as different magnitude of mass movement in each lag time period, the lag time was calculated for the time difference between landslide initiation and peak intensity rainfall

Items	Number of landslide					
Lag time to peak rainfall (h)	−1 to 1	2–3	4–6	7–9	>9	Total
Landslide area <1500 (m^2)	13	8	12	4	9	46
Landslide area 1500–15000 (m^2)	2	1	6	1	6	13
Landslide area >5000 (m^2)	1	2	1	1	6	17
Total	16	11	16	5	15	63

The total number was 63 landslide events during Typhoon Nari.

kind of lag time. Table IV shows the types of landslide case with area exceeding 15,000 m^2. It reveals that the majority of the massive landslides were classified as block slide or circular failure.

It could be concluded that the landslide induced by high intensity rainfall is in smaller magnitude; the main types of mass movement include erosion, debris slide, block slide, and circular failure. Meanwhile, the high accumulation rainfall is relevant strongly to trigger medium to massive landslide.

3. Rainfall Characteristics Analysis

During summer and fall seasons, July–November, Taiwan is threatened by numerous typhoons. The rainfall is following the typhoon cloud-band. The

Table III. Number of counts as events occurred as different classification of mass movement

		Number of landslide						
	Items	Falls	Wedge failure	Plane failure	Erosion	Debris slide	Block slide	Circular failure
Lag time to peak rainfall (h)	−1 to 0	0	0	0	2	2	1	11
	1–3	0	0	2	0	1	2	6
	4–6	0	0	0	2	5	1	8
	7–9	1	0	0	1	0	0	3
	>9	0	1	0	3	1	1	9
	Total	1	1	2	8	9	5	37

The lag time is calculated for the time difference between landslide initiation and peak intensity rainfall. The total number was 63 landslide events during Typhoon Nari.

Table IV. Number of counts as landslide which area exceeding 1500 m^2 occurred as different classification of mass movement

		Number of landslide with area exceeding 1500 m^2						
	Items	Falls	Wedge failure	Plane failure	Erosion	Debris slide	Block slide	Circular failure
Lag time to peak rainfall (h)	−1 to 1	0	0	0	0	0	0	3
	2–3	0	0	1	0	0	1	1
	4–6	0	0	0	0	1	1	2
	7–9	0	0	0	0	0	0	1
	>9	0	1	0	0	0	1	4
	Total	0	1	1	0	1	3	11

The lag time is calculated for the time difference between landslide initiation to peak intensity rainfall. The number of landslide area exceeding 1500 m^2 was 17 of total 63 landslide events during Typhoon Nari.

variance of typhoon path and the width of cloud bands result in different rainfall distribution conditions.

In the study, six paths of typhoon (from year of 1998 to 2002, as shown in Figure 1) were selected including: (1) Typhoon Babs (1998) in the direction of south-west towards to north-west. (2) Typhoon Nakri (2002) in the direction of south-east towards to north-east. (3) Typhoon Bilis (2000) in the direction of south-east towards to south-west. (4) Typhoon Sinlaku (2002) in the direction of north-east towards to north-west. (5) Typhoon Xangsane (2000) in the direction of south-west towards to north-east. (6) Typhoon Nari (2001) in the direction of north-east towards to south-west. Besides the six typhoons, a tropical troposphere event induced torrential

rains on September 5, 2001 was introduced to figure out the rainfall characteristic in Taipei City.

The correlation analysis follows the statistic concepts of cross covariance and cross correlation (Lewis, 1995; Webster and Oliver, 2001).

The cross covariance C_{jk} is defined as:

$$C_{jk}(\tau) = \sum_{i=1}^{N} r_j(t_i) * r_k(t_i + \tau), \tag{1}$$

where C_{jk} is the cross covariance between two rain gauge stations, τ is the time increment or duration (h), r_j is the hourly intensity of the nearest rain gauge station j to the landslide location, r_k is the hourly intensity of the farer rain gauge station k to the landslide location within the scanning radius, t_i is the time of rainfall initiated.

Cross correlation S is a non-dimensional normalized cross covariance (Lewis, 1995; Webster and Oliver, 2001). The parameter of cross correlation is defined as:

$$S_{jk} = \frac{C_{jk}}{\sqrt{C_{jj}C_{kk}}}, \tag{2}$$

where S_{jk} is the cross correlation of the rainfall distribution between two rain gauge stations, C_{jk} is the cross covariance of two rain gauge stations as calculated by Equation (1), C_{jj} and C_{kk} are the cross covariance of station j and k, respectively.

The cross correlation coefficient is limited from 0 to 1. The correlation between two adjacent rain gauge stations depends on the value of cross correlation. Higher the value gets similar two variables assemble. Table V shows an example of the cross correlation coefficients calculated from 14 rain gauge stations for Typhoon Nari in 2001.

The process of rainfall characteristic analysis explains as follow. Rain gauge stations with less correlation are eliminated from the study regions and grouping the stations with similar rainfall characteristic. For Typhoon Nari, three groups of stations are achieved as shown in the shaded part of Table V. Following above process, the selected typhoons and the tropic torrential rainfall event were analyzed. Figure 3 reveals the result of grouped rain gauge stations for each typhoon and one tropical torrential rainfall event.

Rain gauge stations were summarized into three groups eventually as shown in Figure 4. The coverage area of each rain gauge station can be delineated by Thiessen's polygon method in geography information system (GIS). As shown in Figure 4, point P was determined with equal distance to the adjacent three rain gauge stations and then one could delineate polygon of the representing area from rain gauge stations. Each polygon

Table V. Cross correlation coefficients of rainfall stations in Taipei City for Typhoon Nari (2001) event

Station	Zhuzihu	Guandu	Tianmu	Shipal	Shezidao	Shilin	Waishuangxi	Dazhi	Neihu	Nangang	Taipei	Xinyi	Gongguan	Muzha
Zhuzihu	1.000	0.805	0.932	0.920	0.841	0.775	0.765	0.778	0.735	0.698	0.553	0.494	0.224	0.503
Guandu	0.805	1.000	0.812	0.905	0.917	0.826	0.729	0.757	0.704	0.674	0.541	0.468	0.313	0.352
Tianmu	0.932	0.812	1.000	0.972	0.903	0.862	0.862	0.865	0.845	0.776	0.558	0.527	0.287	0.525
Shipal	0.920	0.905	0.972	1.000	0.961	0.910	0.876	0.889	0.858	0.811	0.609	0.566	0.352	0.494
Shezidao	0.841	0.917	0.903	0.961	1.000	0.922	0.844	0.888	0.842	0.815	0.646	0.591	0.431	0.450
Shilin	0.775	0.826	0.862	0.910	0.922	1.000	0.925	0.972	0.938	0.846	0.638	0.579	0.448	0.424
Waishuangxi	0.765	0.729	0.862	0.876	0.844	0.925	1.000	0.922	0.929	0.792	0.511	0.486	0.378	0.339
Dazhi	0.778	0.757	0.865	0.889	0.888	0.972	0.922	1.000	0.973	0.884	0.653	0.613	0.454	0.481
Neihu	0.735	0.704	0.845	0.858	0.842	0.938	0.929	0.973	1.000	0.883	0.593	0.577	0.416	0.463
Nangang	0.698	0.674	0.776	0.811	0.815	0.846	0.792	0.884	0.883	1.000	0.796	0.812	0.601	0.641
Taipei	0.553	0.541	0.558	0.609	0.646	0.638	0.511	0.653	0.593	0.796	1.000	0.956	0.559	0.770
Xinyi	0.494	0.468	0.527	0.566	0.591	0.579	0.486	0.613	0.577	0.812	0.956	1.000	0.588	0.783
Gongguan	0.224	0.313	0.287	0.352	0.431	0.448	0.378	0.454	0.416	0.601	0.559	0.588	1.000	0.395
Muzha	0.503	0.352	0.525	0.494	0.450	0.424	0.339	0.481	0.463	0.641	0.770	0.783	0.395	1.000

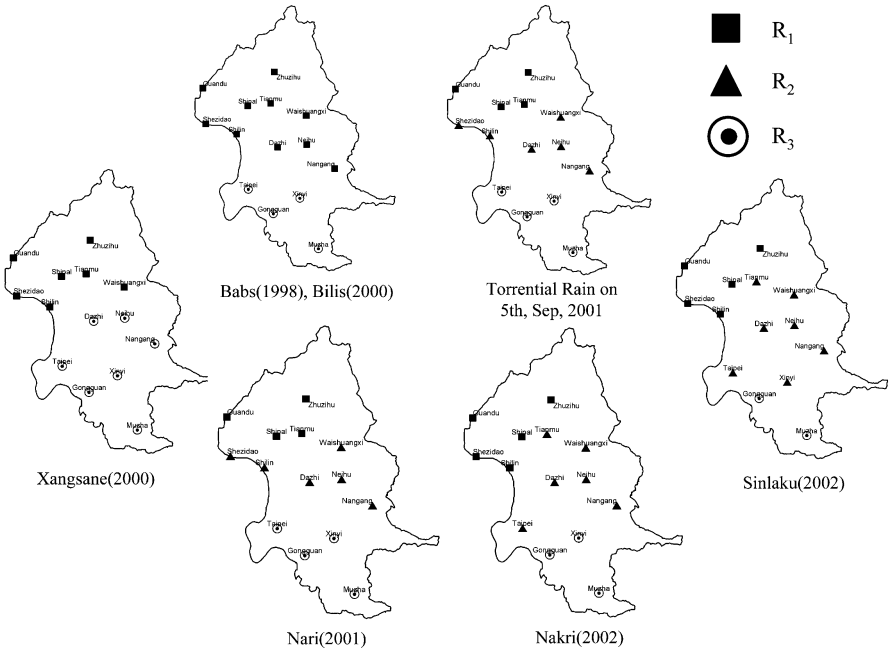

Figure 3. Results of grouped rain gauge stations for each typhoon and one tropic torrential rainfall events. Events included: (1) Typhoon Babs (1998) in the direction of SW towards to NW, (2) Typhoon Nakri (2002) in the direction of SE towards to NE, (3) Typhoon Bilis (2000) in the direction of SE towards to SW, (4) Typhoon Sinlaku (2002) in the direction of NE towards to NW, (5) Typhoon Xangsane (2000) in the direction of SW towards to NE, (6) Typhoon Nari (2001) in the direction of NE towards to SW, and (7) tropic troposphere event induced torrential rains on September 5, 2001.

represents areas having similar rainfall characteristics. Combining the grouped rain gauge stations, Taipei city could be zoned into three sub-regions of rainfall characteristic as shown in Figure 4. The dash line in the figure depicts the three sub-regions, R1, R2, and R3.

4. Geomorphologic Characteristics Analysis

The topography of Taipei City is shown in Figure 5. The aspect of topography follows the tendency of mountain range and distributes in north to west–southwest direction. There are three rivers, Danshui river, Keelung river, and Jingmei stream, flowing the into basin and cutting through the mountain into four individual slopelands. The highest elevation is located in northern Taipei City (T1) in which the elevation varies from 500 to 1100 m. In the middle area (T2), the elevation varies from 400 to 600 m. In the southern area (T3), the elevation varies from 100 to 500 m. In the central area of the basin, a gently alluvial plain was deposited by rivers.

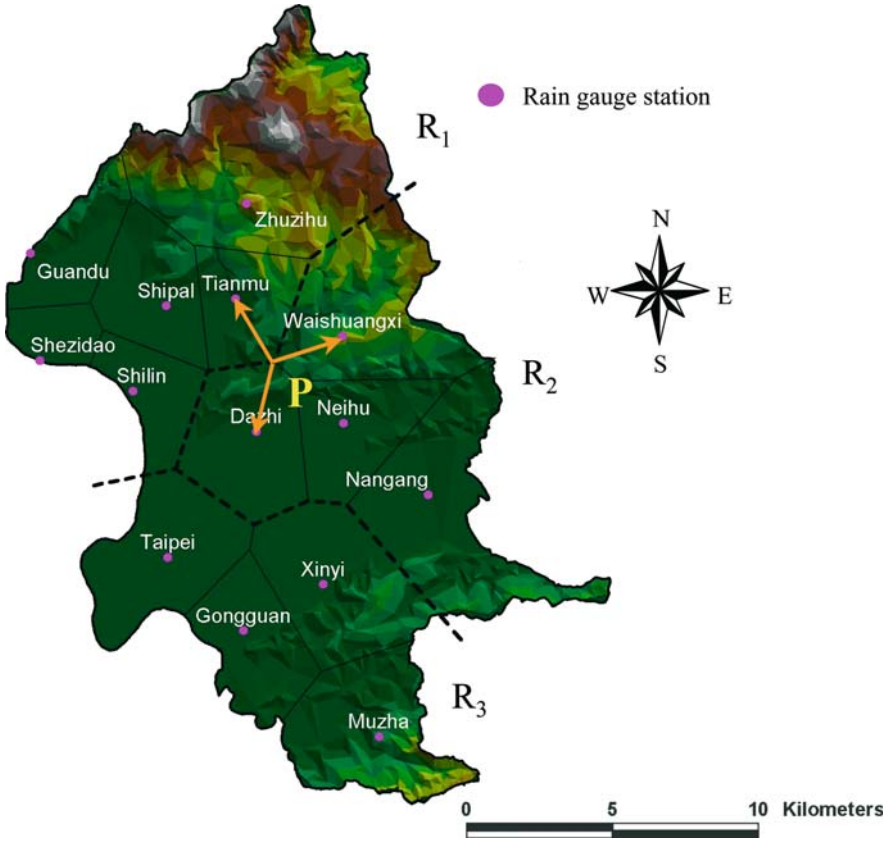

Figure 4. Results of grouped the areas in same rainfall characteristics. Point P was determined with equal distance to the adjacent three rain gauge stations and then one could delineate polygon of the representing area from rain gauge stations. Combining the grouped areas, Taipei City could be zoned into R1, R2, and R3 three sub-regions of same rainfall characteristic.

5. Geological Characteristics Analysis

Taiwan is located at the border between Eurasia and Philippine plates. As a result of the tectonic action, two-thirds of Taiwan belong to the hillsides and are frequently experiencing seismic activities. The simplified geology map in Taiwan is shown in the upper part of Figure 6. The main geology in northmost Taiwan is igneous rock. Sedimentary rock is mainly deposited in the piedmont of west Taiwan. The metamorphic rock is mainly distributed in central and east Taiwan. The geology of Taipei City are shown in the center of Figure 6, the main geology in the north Taipei City is formed by pyroclastic flow and tuff. Both of the middle and the south Taipei City are sedimentary rock mainly. There are four major thrust faults and a series of dip slope structures crossing through the mountain.

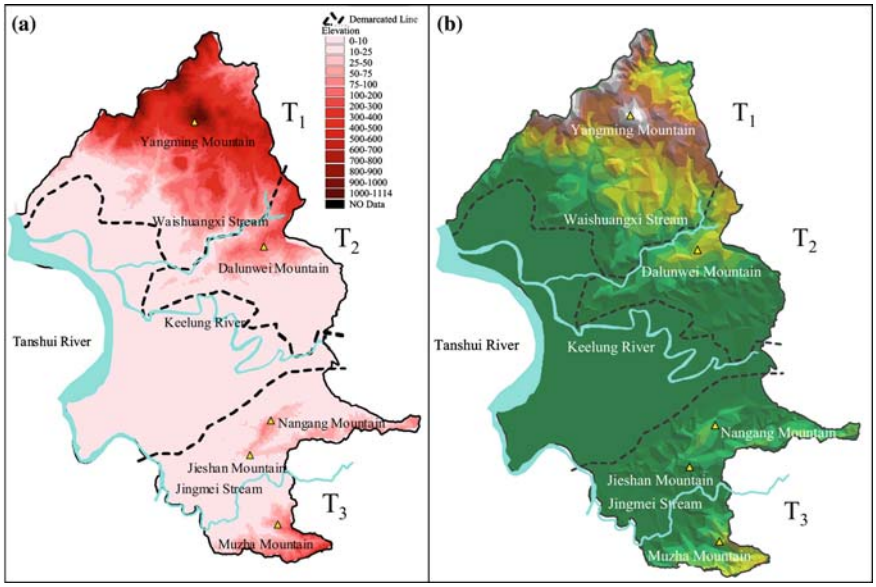

Figure 5. Geomorphologic regionalization map of Taipei City. (a) Identifies the altitude, (b) identifies the aspect.

Dense joints and fissures developed in most rock mass result in weak resistance against weather and erosion.

The geological characteristic classified by the factors of rock strength, the generally unconfined compression strengths identified by Hsu (1983) and Weng (2002) as shown in Table VI. On the basis of type and strength factors, Taipei City could be divided into igneous rock, I (Andesite and Tuff Braccia); sedimentary rock, S1 (Wuchin-shan, Mu-shan, and Taliao); sedimentary rock, S2 (Shihti, Nankang, and Nan-chuang); alluvium, A; four sub-regions as shown in Figure 6. The sedimentary rock region were subdivided into two stratums, S1 is the older stratum located in the north of Keelung River area, S2 is the younger stratum located in the south of Keelung River area.

6. Process for Landslide Regionalization

A flowchart diagram for landslide regionalization analysis is proposed in Figure 7, which introduces the analyses of rainfall, geomorphology and geologic characteristics. Because rainfall is the main trigger of landslide, the rainfall characteristics are prioritized in the landslide regionalization. The result is acts as the base map for the following overlap analysis.

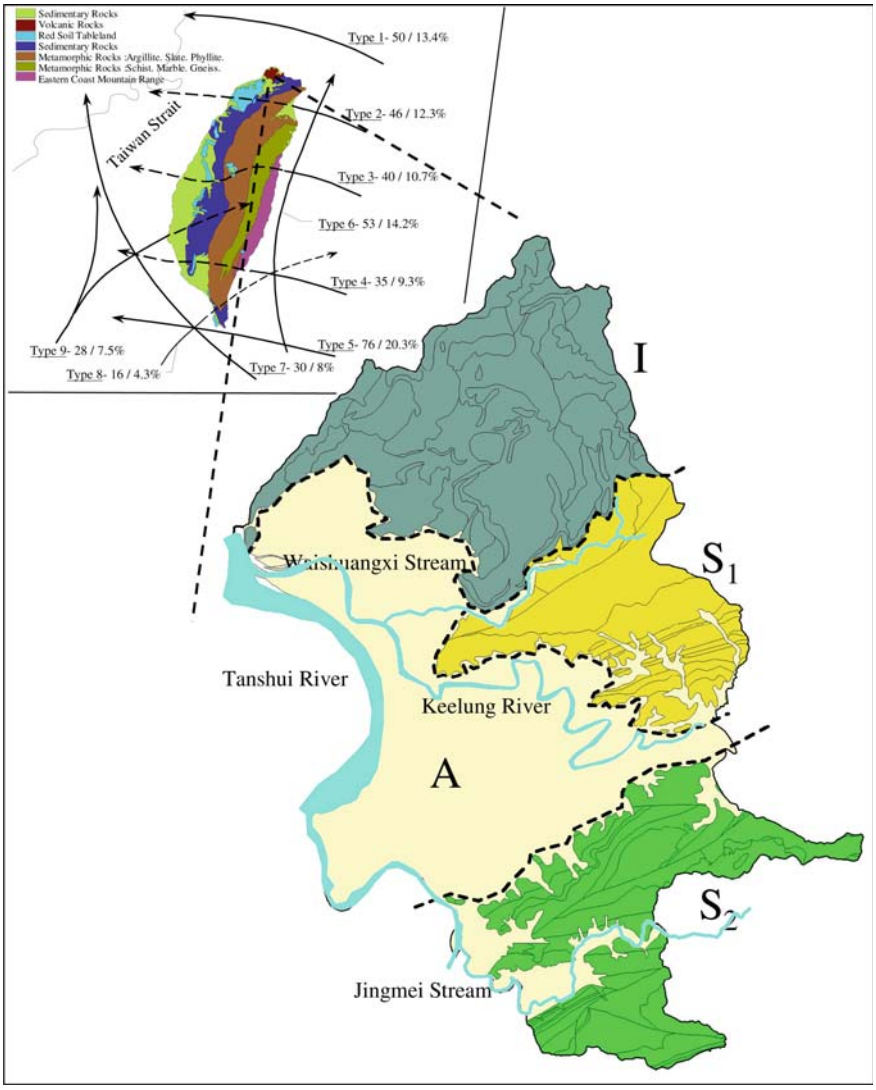

Figure 6. Geologic regionalization map of Taipei city. Integrated the consideration of type and strength factors, Taipei City could be divided into igneous rock, I (Andesite and Tuff Braccia); sedimentary rock, S1 (Wuchin-shan, Mu-shan, and Taliao); sedimentary rock, S2 (Shihti, Nankang, and Nan-chuang); alluvium, A. The simplified geology conditions and various typhoon paths in Taiwan are presented in the upper part of the map.

The second stage considers the geomorphologic characteristics by excluding the gentle slope areas and regionalizing the area by terrain elevation, aspect, as well as other variables. The regionalization is based on the

Table VI. Generally unconfined compression strengths for rocks (Hsu, 1983; Weng, 2002)

Region	Igneous rock		Sedimentary rock						Alluvium
Formation	Andesite	Tuff Braccia	Wuchin shan	Mushan	Taliao	Shithi	Nan-kang	Nan-chuang	Sand and clay
Generally unconfined compression strengths	800 to 1500	1000	350 to 850	300 to 650	210 to 600	140 to 640	100 to 400	15 to 50	< 10

Units: MPa.

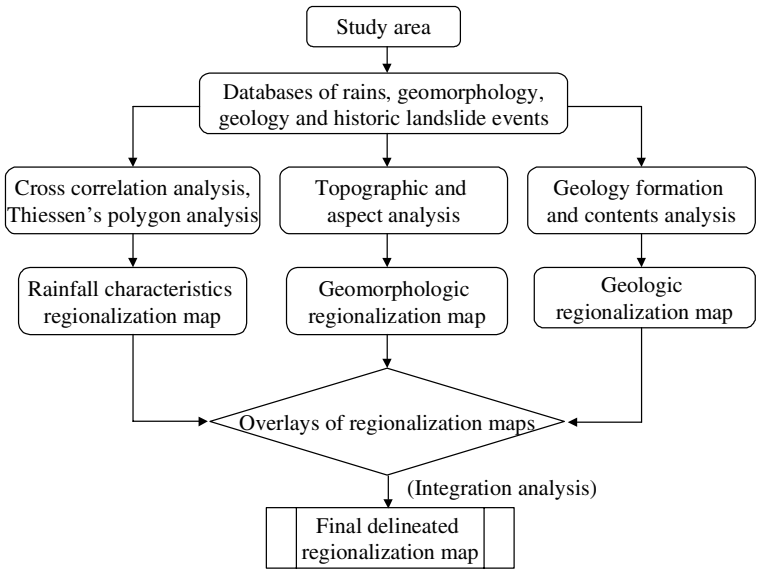

Figure 7. Flow chart for the proposed landslide regionalization process.

variation or discontinuity of factors to delineate out the same characteristic region. The third stage considers the geologic conditions by the formation, strength, etc.

It should be noted that it is possible to have inconsistent boundaries among three analyses. The rainfall characteristic analysis results from interpolation using universal kriging in GIS spatial analysis. It is a process to extend point rainfall records into area distribution data. The analysis of geomorphology or geologic characteristics is based on rigorous field surveying, which has less variance. Consequently, the regionalized results by the geomorphologic and geologic characteristics analyses are more

critical than result by the rainfall characteristic analysis when there are inconsistent sub-region boundaries among three analyses.

By summarizing the above results and excluding the plain areas, the final delimited regionalization map could be divided into N (North), C (Central), and S (South) three sub-regions as presented in Figure 8.

7. Verification for Landslide Regionalization

Landslide data in Taipei City caused by Typhoon Nari in year 2001 was utilized to verify the regionalization result. Distributions of landslides are illustrated in Figure 8. Allocating landslides data into each sub-region reveals

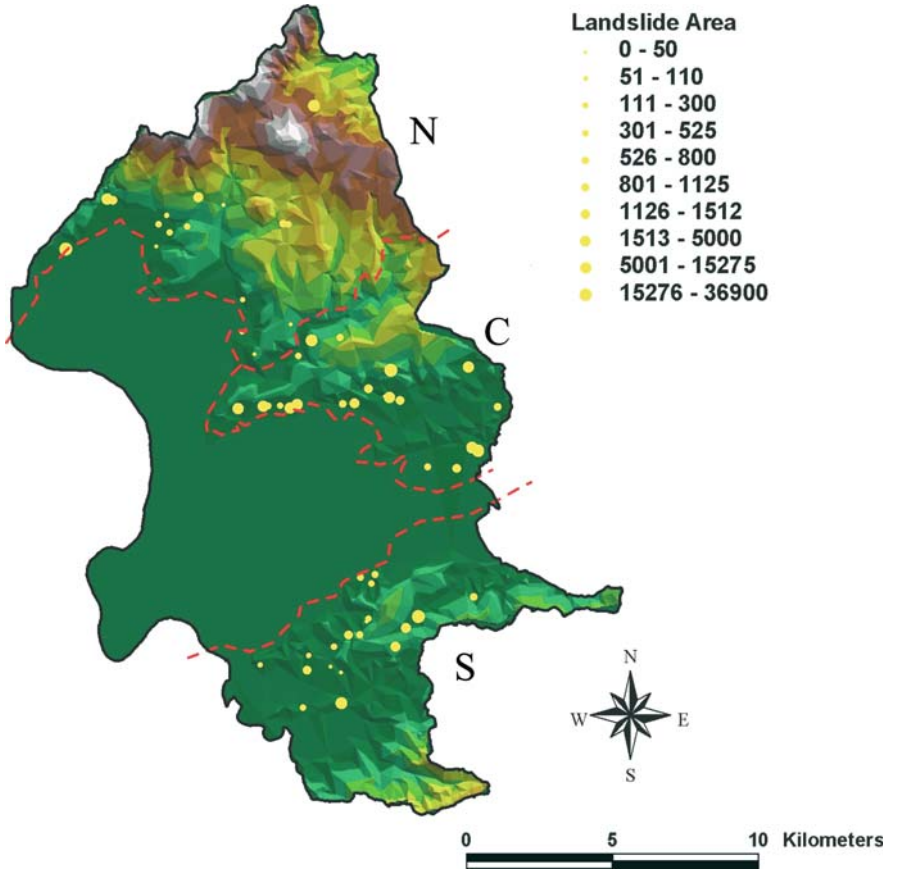

Figure 8. Landslide regionalization map of Taipei City and 63 landslide locations that initiated during Typhoon Nari in year 2001. Summarizing the results of rainfall, geomorphology, and geologic characteristics analyses, Taipei City could be divided into N (North), C (Central), and S (South) three sub-regions. Each sub-region has the same rainfall and landslide characteristics.

that there are 17, 24, and 22 landslides located in the north, central, and south regions, respectively. Each accumulation and intensity rainfall of landslide-initiating are speculated from the rain gauge stations records as mentioned before. For comparison, events data in the same region were grouped. The result is shown in Figure 9. There are four black lines shown in the upper part of the figure, each one shown representing the least square regression line for cases of landslide events in all Taipei City, events in N region, events in C region, and events in S regions, respectively. The result is also illustrated into an area with the least square regression lines minus 1 standard deviation ($\mu - 1\sigma$) as shown in the center part of Figure 9. Each zone represents the distribution of landslide events in a sub-region. Summarizing the results reveal that the data distribution of the sub-region shows more dense than the one for all-region. The distribution characteristic for each sub-region is individual. Figure 9 illustrated the unique landslide characteristic for each sub-region and demonstrated the applicability of regionalization method.

8. Conclusions

Landslide events induced by rainfall were analyzed to figure out the landslide characteristics in Taipei City. The landslide characteristic analyses

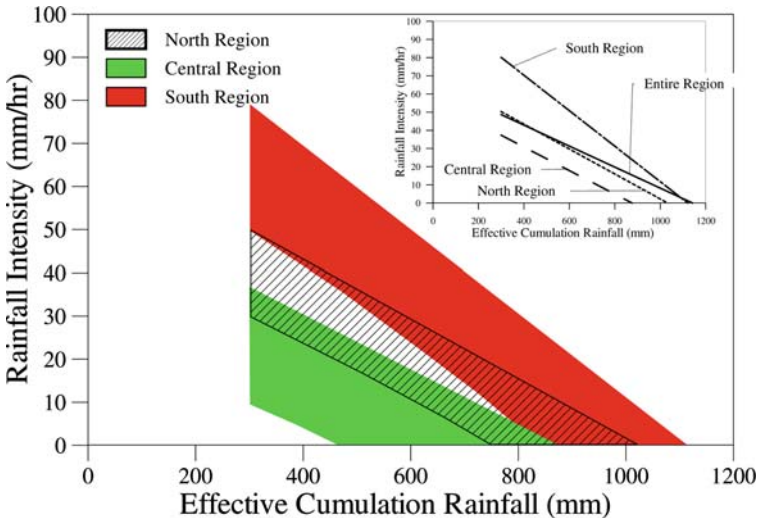

Figure 9. Least square lines and the area of −1 standard deviation ($\mu - 1\sigma$, shaded, lower and upper areas) for landslide located in the north (N), central (C) and south (S) regions in Taipei City, respectively. There are four black lines shown in the upper part of the figure, each one represents the least square regression line for cases of landslide events in all Taipei City, events in the north (N), central (C) and south (S) regions, respectively.

reveal that landslides induced by high intensity rainfall are mainly in smaller magnitude of erosion, debris slide, block slide or circular failure. It is also concluded that the occurrence of massive landslides are associated with higher cumulative rainfall.

Moreover, a regionalization method for landslide was proposed. The regionalization method bases on the regional rainfall, geomorphology, and geologic characteristics considerations. By verifying with the landslide events occurred in Taipei City, the result of proposed process show good agreement with landslide events observed in the Taipei City during Typhoon Nari.

Acknowledgements

This research was supported by the National Science Council, Project number: NSC92-2811-Z-002. The Taipei City government provided part of the data used in this research. Their help is gratefully acknowledged.

References

Ba Mamoudou, B. and Sharon, E. N.: 1998, GOES Multispectral Rainfall Algorithm (GMSRA), *J. Appl. Meteorol.* **40**, 1500–1514.

Caine, N.: 1980, The rainfall intensity duration control of shallow landslides and debris flow, *Geografiska Annaler* **62**, 23–27.

Cannon, S. H. and Ellen, S. D.: 1985, Rainfall conditions for abundant debris avalanches in San Francisco Bay, California, *California Geology* **38**(12), 267–272.

Fan, C. C., Liu, J. C., and Tai, Y. T.: 2002, *Pre-warning Model for Debris Flow Triggering Rainfall and Conductibility of Ground Water*, Report for Bureau of Soil and Water Conservation (in Chinese).

Hsu, T. L.: 1983, *Geology and Engineering*, Society of China Engineer (in Chinese).

Jan, C. D.: 2002, *Pre-warning Model for Debris Flow Triggering Rainfall*, Report for Bureau of Soil and Water Conservation (in Chinese).

Keefer, D. K., Wilson, R. C., Mark, R. K., Brab, E. E., Brown, W. M., Ellen, S. D., Harp, E. L., Wieczorek, G. F., Alger, C. S., and Zatkin, R. S.: 1987, Real-time landslide warning during heavy rainfall,, *Science* **238**, 921–925.

Lewis, J. P.: 1995, Fast Template Matching, *Proceedings Vision Interface, 95*, Quebec, May 120–123.

Singhroy, V., Mattar, K. E., and Gray, A. L.: 1998, Landslide characterisation in Canada using interferometric SAR and combined SAR and TM images, *Adv. Space. Res.* **21**(3), 465–476.

Sugiyama, T., Okada, K., Muraishi, H., Noguchi, T., and Samizo, M.: 1995, Statistical rainfall risk estimating method for a deep collapse of a cut slope, *Soils and Foundations* **35**(4), 37–48.

Webster, R. and Oliver, M.: 2001, *Geostatistics for Environmental Scientists*, John Wiley and Sons, Chichester, England, pp. 149–192.

Weng, M. C.: 2002, Mechanics property and microscopic structure characteristics of weak sandstone, PhD Thesis, National Taiwan University, Taiwan (in Chinese).

Wieczorek, G. F.: 1987, Effect of rainfall intensity and duration on debris flows in Central Santa Cruz Mountains, California flows/avalanches process, recognition and mitigation, Geological Society of America, *Rev. Eng. Geol.* **7**, 93–104.